Bridging the Digital Divide Using SuperCell Massive MIMO

Unnikrishnan Kunnath Ganesan, Emil Björnson and Erik G. Larsson

Kunnath Ganesan, U., Björnson, E., Larsson, E. G., (2022), Bridging the Digital Divide Using SuperCell Massive MIMO, *2022 IEEE 96th Vehicular Technology Conference (VTC2022-Fall)*.
https://doi.org/10.1109/VTC2022-Fall57202.2022.10012724

Original publication available at:
https://doi.org/10.1109/VTC2022-Fall57202.2022.10012724

Bridging the Digital Divide Using SuperCell Massive MIMO

Unnikrishnan Kunnath Ganesan*, Emil Björnson† and Erik G. Larsson*
*Department of Electrical Engineering (ISY), Linköping University, Linköping, Sweden.
Emails: {unnikrishnan.kunnath.ganesan, erik.g.larsson}@liu.se
†Division of Communication Systems, KTH Royal Institute of Technology, Stockholm, Sweden.
Email: emilbjo@kth.se

***Abstract*—Massive multiple input multiple output (MIMO) emerged as the leading technology for supporting fifth generation (5G) and beyond 5G cellular communication systems. Due to the tremendous increase in data traffic in urban areas and to meet such a significant demand, most studies consider macro/micro cell deployments in urban environments. Internet service providers (ISPs) are less interested in providing communication services in rural areas considering the relatively low profits compared to the deployment and maintenance costs. In this paper, we investigate the massive MIMO performance in rural scenarios. In particular, we investigate different aspects to consider while designing a long-range communication system. We propose to use elevated base station (BS) with sectorized antennas with unusually large aperture and implement a user scheduling algorithm at the BS to provide full digital coverage. We analyze the coverage range of a massive MIMO system to provide high-rate services. Furthermore, we also analyze the link budget requirements and the rates users can achieve in such a SuperCell massive MIMO network.**

***Index Terms*—Massive MIMO, SuperCell, digital divide, scalability, coverage.**

I. Introduction

Massive multiple input multiple output (MIMO), since its inception in [1], has grown into the leading physical-layer technology for fifth generation (5G) and beyond wireless networks. Massive MIMO utilizes many antennas at the base station (BS) to serve many terminals simultaneously, in the same time-frequency resource, thereby improving the throughput and traffic capacity of the radio link. Massive MIMO has been mainly studied for providing services in urban or suburban areas. Currently, there is a huge imbalance between the broadband services enjoyed in urban and rural areas in many countries. A major issue is the revenue; most internet service providers (ISPs) consider users per cell as too low in the rural areas and thus the return on investment against the cost of building infrastructure and maintenance, is too small. However, as the world becomes increasingly digitized, broadband services are becoming a necessity and we need to develop technology that can bridge the digital divide between urban developed regions and underdeveloped rural regions [2]. In addition to voice connectivity, rural areas can make efficient use of digital technologies for smart schooling, smart agriculture, e-health, and climate monitoring helping the people to progress on education, health, and business levels [3], [4]. In the survey paper [4], it was pointed out that there is no single optimal solution that can provide ubiquitous global connectivity. Moreover, each rural area comes with its own challenges, for example, the availability of a local power grid.

This work is supported in part by ELLIIT and in part by Swedish Research Council (VR) and in part by KAW foundation.

Usage of high-gain, high-order sectorized antennas on tall towers as a wide area coverage solution is proposed in [5] with Luneberg lenses [6] and array panels as candidate antenna solutions for SuperCell requirements. The paper [7] posed the problem of extended coverage for 6G using massive MIMO. A case study on fixed broadband access in rural areas with coverage up to 12 km is made in [8, Ch. 6]. Usage of highly sectorized antennas deployed at existing TV towers of height 250 m providing coverage up to 70 km was suggested in [9] assuming the channel fading model as Rayleigh. Small scale fading occurs in wireless communications due to the existence of multi-path components. However, the multi-path profile depends on the distance between the BS and the user as well as the environment in the vicinity. Thus, with an elevated BS and long-distance users, the multi-path profile will be limited to a small angle dispersion in azimuth and elevation planes. The scattering will be limited near the users and assuming independent and identically distributed (i.i.d). Rayleigh is not suitable for long-distance communication scenarios.

There are rural parts of developing countries that lack good cellular coverage and capacity since a market-driven deployment would cost more than the inhabitants can afford. However, the UN sustainability goals require us to bridge the digital divide. In this paper, we study different aspects of massive MIMO for the support of long-distance communication. We consider an elevated BS at heights at least 100 m above the ground to serve a geographically large cell. We call this concept SuperCell massive MIMO. We provide a feasibility study showing that a sparse deployment of tall masts with SuperCells can solve the coverage/capacity issue. It should therefore be considered by entities that explores how to bridge the digital divide in the least cost-inefficient way. The contributions of our paper are as follows:

1) We use a cluster-based channel model considering local scattering near the user terminals for studying long-

distance communications using an elevated BS.
2) We investigate different aspects to consider in the system design and the link budget requirements for long distance communications.
3) We study the requirement of minimum separation among the users so that the BS can resolve the channels.
4) We provide a user scheduling algorithm to deal with users whose channel vectors are nearly parallel.

Notations: Bold lowercase letters are used to denote vectors and bold uppercase letters are used to denote matrices. $\mathbb{C}$ denotes the set of complex numbers. For a matrix $\mathbf{A}$, $\mathbf{A}^*$, $\mathbf{A}^{\mathrm{T}}$ and $\mathbf{A}^{\mathrm{H}}$ denote conjugate, transpose and conjugate transpose of the matrix $\mathbf{A}$ respectively. $\mathcal{CN}(0,\sigma^2)$ denotes a circularly symmetric complex Gaussian random variable with zero mean and variance equal to σ^2. $\mathrm{Tr}(\mathbf{A})$ denotes the trace of $\mathbf{A}$. The identity matrix of size $N\times N$ is denoted by $\mathbf{I}_N$. $\mathrm{Vec}(\cdot)$ denotes the vectorizing operator.

II. System Modeling and Analysis

We consider a single-cell system with a BS in the middle of the cell serving K single-antenna user equipments (UEs). The BS is elevated by mounting it on a tall tower or a mountain, providing a height h_b above the ground level and is equipped with P panels with each panel consisting of a uniform planar array (UPA) with $H\times V$ antennas. The total number of antenna elements at the BS is $M = PHV$. In any arbitrary coherence block, let $\mathbf{g}_k \in \mathbb{C}^{M\times 1}$ be the channel from UE k to the BS. Let $\mathbf{G} = [\mathbf{g}_1\ \mathbf{g}_2 \dots\ \mathbf{g}_K] \in \mathbb{C}^{M\times K}$ be the overall channel matrix. In this paper, we use Cartesian coordinates (x,y,z) and its corresponding polar coordinates (d,θ,φ), interchangeably. The one-to-one mapping between the Cartesian and the polar coordinate systems is given by

$$[x\ y\ z]^{\mathrm{T}} = d[\cos(\theta)\cos(\varphi)\quad \cos(\theta)\sin(\varphi)\quad \sin(\theta)]^{\mathrm{T}}. \quad (1)$$

A. Channel Model

In this subsection, we discuss the channel modeling for long range scenarios. Let the center of the BS be at the point $(0,0,h_b)$. Consider a single UE located at $(d,\bar{\theta},\bar{\varphi})$ and let the corresponding channel be $\mathbf{g} = [g_1\ g_2\ \dots\ g_M]^{\mathrm{T}} \in \mathbb{C}^{M\times 1}$. In this paper, we consider that the BS is equipped with directional micro-strip patch antennas [10], [11].

1) Cluster-Based Channel Modeling: With an elevated BS and the UEs at very large distances, a rich scattering environment may not be available. As the BS is elevated we assume that there are no scatterers around the BS. However, there might be local scattering around the UEs, thus we need a model to capture that [12]. Consider N_{cl} clusters around the UE which are distributed in a clustering radius of r. Let cluster n be located at (d_n,θ_n,φ_n). Let $\mathbf{u}_m \in \mathbb{R}^3$ be the location of the m^{th} antenna at the BS. The channel g_m between the mth BS antenna and the UE can be written as

$$g_m = \sqrt{G_m(\bar{\varphi},\bar{\theta})\mathrm{PL}(d)}e^{-\frac{j2\pi d}{\lambda}}e^{j\mathbf{k}(\bar{\varphi},\bar{\theta})^T\mathbf{u}_m} + \sum_{n=1}^{N_{cl}}\sqrt{G_m(\varphi_n,\theta_n)\mathrm{PL}(d_n)\mathrm{PL}(d_{n0})\mathrm{CG}_n}Z_n e^{j\mathbf{k}(\varphi_n,\theta_n)^T\mathbf{u}_m}, \quad (2)$$

where $G_m(\varphi,\theta)$ is the directional gain from the mth antenna in the direction of (φ,θ), d_{n0} denotes the distance between the UE and cluster n, CG_n denotes the cluster dependent gain parameter which includes the radar cross section and $Z_n \sim \mathcal{CN}(0,1)$ captures the small-scale fading associated with the cluster. The vector $\mathbf{k}(\varphi,\theta) = \frac{2\pi}{\lambda}[\cos(\theta)\cos(\varphi)\ \ \cos(\theta)\sin(\varphi)\ \ \sin(\theta)]^{\mathrm{T}}$ is the wave vector of a plane wave with wavelength λ that impinges on the antenna array under the azimuth angle φ and the elevation angle θ. The first term in (2) represents the direct line-of-sight (LoS) channel and the second term refers to the channel gain from N_{cl} clusters. When the UEs are located far away, the angular interval from which the signal is coming from each cluster will be tiny. Thus, the antenna gain variations for all the antenna elements belonging to single UPA panel p will be negligible in the angular interval. Thus, we assume that the directional antenna gain is the same for a panel p and, hence, the channel vector $\mathbf{g}_{\mathrm{p}} \in \mathbb{C}^{HV\times 1}$ is

$$\mathbf{g}_{\mathrm{p}} = \sqrt{G_{\mathrm{p}}(\bar{\varphi},\bar{\theta})\mathrm{PL}(d)}e^{-\frac{j2\pi d}{\lambda}}\mathbf{a}(\bar{\varphi},\bar{\theta}) + \sum_{n=1}^{N_{cl}}\sqrt{G_{\mathrm{p}}(\varphi_n,\theta_n)\mathrm{PL}(d_n)\mathrm{PL}(d_{n0})\mathrm{CG}_n}Z_n\mathbf{a}(\varphi_n,\theta_n), \quad (3)$$

where $\mathbf{a}(\cdot,\cdot)$ is the array response vector of the panel.

2) Pathloss Model: In this paper, we use the Ericsson 9999 pathloss model for long-distance communications [13] and consider the typical 5G band at 3.5 GHz. Let h_r be the height of the UE. Let d be the distance between the BS and the UE. Let f be the frequency of operation. The Ericsson 9999 pathloss model [13], [14] is given by

$$\begin{aligned}\mathrm{PL(dB)} =& 51.5 + \left(34 + 0.1\log_{10}\left(\frac{h_b}{1\text{ m}}\right)\right)\log_{10}\left(\frac{d}{1\text{ km}}\right) \\ &- 12\log_{10}\left(\frac{h_b}{1\text{ m}}\right) - 3.2\left(\log_{10}\left(11.75\left(\frac{h_r}{1\text{ m}}\right)\right)\right)^2 \\ &+ 44.49\log_{10}\left(\frac{f}{1\text{ MHz}}\right) - 4.78\left(\log_{10}\left(\frac{f}{1\text{ MHz}}\right)\right)^2. \end{aligned} \quad (4)$$

B. Channel Estimation

Let τ_c be the length of the coherence interval and $\tau_p < \tau_c$ be the length of the pilot signal from the UEs. Let $\boldsymbol{\phi}_k \in \mathbb{C}^{\tau_p\times 1}$ be the pilot signal associated with UE k such that $\boldsymbol{\phi}_k^{\mathrm{H}}\boldsymbol{\phi}_k = 1$. Due to the low mobility of the UEs, we could allocate orthogonal pilot sequences to all the UEs, i.e., $\boldsymbol{\phi}_k^{\mathrm{H}}\boldsymbol{\phi}_{k'} = 0$ for $k \neq k'$. Let $\boldsymbol{\Phi} = [\boldsymbol{\phi}_1\ \boldsymbol{\phi}_2\ \dots\ \boldsymbol{\phi}_K] \in \mathbb{C}^{\tau_p\times K}$ be a matrix that contains the pilot signals for all UEs. From the above assumptions, we have $\boldsymbol{\Phi}^{\mathrm{H}}\boldsymbol{\Phi} = \mathbf{I}_K$. In the channel estimation phase, all UEs transmit their pilot signals and the signal received at the BS $\mathbf{Y}_{\mathrm{p}} \in \mathbb{C}^{M\times\tau_p}$ is given by

$$\mathbf{Y}_{\mathrm{p}} = \sqrt{\tau_{\mathrm{p}}\rho_{\mathrm{ul}}}\mathbf{G}\boldsymbol{\Phi}^{\mathrm{H}} + \mathbf{W}_{\mathrm{p}}, \quad (5)$$

where ρ_{ul} is the uplink transmit power and $\mathbf{W}_p$ is additive white Gaussian noise (AWGN) with i.i.d. $\mathcal{CN}(0,\sigma^2)$ entries and σ^2 is the noise power. It is hard to obtain channel statistics due to high computational complexity and the need to store

huge matrices. Thus, in this paper we consider least-squares channel estimates and is given by

$$\hat{\mathbf{G}}_{\text{LS}} = \frac{\mathbf{Y}_{\text{p}}\mathbf{\Phi}}{\sqrt{\tau_{\text{p}}\rho_{\text{ul}}}}. \tag{6}$$

C. Downlink Spectral Efficiency

Here we consider the rates achieved by the UEs of the SuperCell system in the presence of interference from other UEs. The collective signals received by all the UEs in the downlink can be collected into a single vector and is given by

$$\mathbf{y} = \sqrt{\rho_{\text{dl}}}\mathbf{G}^{\text{H}}\mathbf{x} + \mathbf{w}, \tag{7}$$

where $\mathbf{x} \in \mathbb{C}^{M\times 1}$ is the signal transmitted by the BS to all UEs and $\mathbf{w}$ is the AWGN with i.i.d. $\mathcal{CN}(0, \sigma^2)$ entries. Let $\mathbf{V}$ be the precoding matrix such that

$$\mathbf{x} = \mathbf{V}\mathbf{q}, \tag{8}$$

where $\mathbf{q} = [q_1\ q_2\ \ldots\ q_K]^{\text{T}} \in \mathbb{C}^{K\times 1}$ and q_k is the signal intended for the kth UE. The received signal at UE k is then given by

$$y_k = \sqrt{\rho_{\text{dl}}}\sum_{i=1}^{K}\mathbf{g}_k^{\text{H}}\mathbf{v}_i q_i + w_k, \tag{9}$$

which can be equivalently written as

$$\begin{aligned} y_k =& \sqrt{\rho_{\text{dl}}}\mathbb{E}\left\{\mathbf{g}_k^{\text{H}}\mathbf{v}_k\right\} q_k + \sqrt{\rho_{\text{dl}}}\left(\mathbf{g}_k^{\text{H}}\mathbf{v}_k - \mathbb{E}\left\{\mathbf{g}_k^{\text{H}}\mathbf{v}_k\right\}\right) q_k \\ &+ \sqrt{\rho_{\text{dl}}}\sum_{i=1, i\neq k}^{K}\mathbf{g}_k^{\text{H}}\mathbf{v}_i q_i + w_k. \end{aligned} \tag{10}$$

The effective signal-to-interference-plus-noise ratio (SINR) at UE k, using use-and-then-forget bound [8, Sec. 2.3.4], can be written as

$$\text{SINR}_k = \frac{\rho_{\text{dl}}\left|\mathbb{E}\left\{\mathbf{g}_k^{\text{H}}\mathbf{v}_k\right\}\right|^2}{\sigma^2 + \rho_{\text{dl}}\sum_{i=1, i\neq k}^{K}\mathbb{E}\left\{\left|\mathbf{g}_k^{\text{H}}\mathbf{v}_i\right|^2\right\} + \rho_{\text{dl}}\text{var}\left\{\mathbf{g}_k^{\text{H}}\mathbf{v}_k\right\}}. \tag{11}$$

The net spectral efficiency (SE) of UE k is

$$\text{SE}_k = \left(1 - \frac{\tau_p}{\tau_c}\right)\log_2\left(1 + \text{SINR}_k\right). \tag{12}$$

III. Aspects to Consider In The SuperCell System

In this section, we discuss certain aspects of long-distance communication which need to be considered while modeling the system parameters.

A. Scaling Loss

In this subsection we study the losses in the performance of a massive MIMO system with scaling of distance. Suppose we have a single cell with a BS consisting of M antennas and K UEs randomly distributed in the cell. The SINR in downlink with i.i.d. Rayliegh fading and a max-min fairness power control policy is given by [8, Table 5.4]

$$\overline{\text{SINR}} = \frac{M\rho_{\text{dl}}}{\sum_{k=1}^{K}\frac{1}{\beta_k}} \tag{13}$$

where ρ_{dl} is the downlink transmit power and β_k is the channel gain associated with the UE k. In (13), perfect channel state information and maximum ratio precoding are assumed.

Let the pathloss exponent be η. For every doubling of the cell radius, the pathloss will increase by 2^η times. Hence, on average to keep the rates given to the UEs the same when the cell size increases, the number of antennas at the BS need to be increased by 2^η times. Moreover, if we intend to provide the same rate per UE and constant UE density, the number of UEs will quadruple when doubling the cell radius. Thus, to provide same rates to UEs/area, the number of BS antennas or the downlink transmit power needs to be increased by $4 \cdot 2^\eta$ times for every doubling of the cell radius. Considering an approximate value of the pathloss exponent $\eta = 3.5$ from (4), the increment should be done by 44 times.

B. LoS Distance over the Earth's Horizon

The LoS distance which can be seen above the horizon when using a BS of height h_b is approximately given by

$$d_{\text{LoS}} = \sqrt{2Rh_b} \tag{14}$$

where $R = 6371$ km is the radius of the earth. The typical range over which an elevated BS can see a UE is tabulated in Table I. Thus, to provide long-distance communications we need to deploy sufficiently highly elevated BS. Moreover, from (4) with the increase in the height of the BS, the pathloss also increases. However, building a BS that holds thousands of antenna elements at huge heights is not easy. We need to consider the structural stability against the wind at those heights, but this is out of scope of this discussion.

TABLE I: LoS distances over the earth horizon for different BS heights.

BS height (h_b) (m)	LoS distance (d_{LoS}) (km)
100	35.7
150	43.73
300	64.84

C. Minimum Separation between users

As we consider an elevated BS for the SuperCell massive MIMO network, the channel seen by the BS from the UEs will be predominantly LoS. As the UEs are located very far from the BS, it can happen that the channels of multiple UEs fall in the main lobe of the signal transmitted from the BS. If this happens, then the channel vectors from those UEs will be nearly parallel and, thus, the BS will be unable to distinguish them. This can lead to severe interference and the rates will get severely degraded. Thus, it is very important in a long-distance communication scenario that the UEs does not fall in the same main lobe from the BS. In this section, we discuss the minimum separation required among the UEs.

Consider two UEs at the same distance separated only in the azimuth plane and located at a distance R from the BS. Without loss of generality, consider UEs at locations (R, φ_1, θ) and (R, φ_2, θ). Their corresponding array response vectors at

the BS are given by $\mathbf{a}_1(\varphi_1, \theta)$ and $\mathbf{a}_2(\varphi_2, \theta)$, respectively. The two array responses are orthogonal if $\mathbf{a}_1^{\mathrm{H}}\mathbf{a}_2 = 0$. Thus,

$$\sum_{h=1}^{H}\sum_{v=1}^{V} e^{j2\pi\Delta_h(h-1)(\sin\varphi_2-\sin\varphi_1)\cos\theta} = 0 \quad (15)$$

$$\implies V\frac{e^{j2\pi\Delta_h H(\sin\varphi_2-\sin\varphi_1)\cos\theta}-1}{e^{j\pi(\sin\varphi_2-\sin\varphi_1)\cos\theta}-1} = 0 \quad (16)$$

$$\implies e^{j2\pi\Delta_h H(\sin\varphi_2-\sin\varphi_1)\cos\theta} = 1. \quad (17)$$

Considering $\theta = 0$ (this can be motivated by the fact that, for long distance communications, the variation in elevation angle will be very small or the antenna panel can be tilted such that the elevation angle to the UE is zero) and without loss of generality, let $\varphi_1 = 0$ and $\varphi_2 = \Delta\varphi$, where $\Delta\varphi$ is the minimum angular separation between two UEs such that, the array responses are orthogonal. Thus, by solving (17) we get

$$\sin\Delta\varphi = \frac{1}{\Delta_h H}. \quad (18)$$

Thus, the minumum separation (d) between the UEs in the azimuth plane for the UEs at distance of D is given by

$$d = 2D\sin\left(\frac{\Delta\varphi}{2}\right). \quad (19)$$

For $H = 100$ antennas, $\Delta_h = 2$ and at a distance $D = 40$ km, the minimum separation between the UEs to have orthogonal array responses (in a LoS scenario) is $d = 200$ m.

Similar to the azimuth case, the minimum angular separation required in the elevation plane is given by

$$\sin\Delta\theta = \frac{1}{\Delta_v V}. \quad (20)$$

D. Types of Targeted Users

Considering an isotropic antenna at a distance of 40 km from the BS, the signal will encounter a pathloss of around 170 dB when using the model in (4). With 100 MHz bandwidth and a noise figure of 7 dB, the noise power level is -116 dB. We need to have a certain signal-to-noise ratio (SNR) target for channel estimation to provide the benefits of massive MIMO. Thus, for the BS to estimate the channel for a UE at 40 km distance, the high pathloss need to be compensated for by the means of uplink power, directional antenna gain at the UE and pilot length for integration. A mobile handset usually has antenna gains of around 0 dBi and transmits in all directions and use rather low power (around 500 mW with a class-2 power amplifier) compared to BS. Thus, to compensate from the power disparity between uplink pilots and downlink transmission, we need to have very large pilot lengths, which again is an infeasible option as it reduces the spectral efficiency of the system.

A fixed wireless access (FWA) terminal can transmit at high powers and since the FWA is not mobile, the channel remains relatively constant for a very long time providing a longer coherence interval. Moreover, FWA can be deployed with directional antennas facing towards the BS as well and it can be deployed at elevated heights, thereby helping to reduce the pathloss further. Also, FWA can act as a router which connects to mobile handsets in a small local network. Thus, FWA connected to the electricity grid is more feasible in long distance scenario.

Algorithm 1: User scheduling algorithm.

Input: $\hat{\mathbf{G}}$ and γ_{th}.
Initialize: $\mathcal{K}_0 = \mathcal{K}$, $j = 1$.
Compute $\mathbf{\Gamma} = [\gamma_{kk'}] \quad \forall\ (k, k')$.
while $k \in \mathcal{K}_0$ **do**
  $\mathcal{K}_j = \{k' : \gamma_{kk'} > \gamma_{\text{th}}\}$
  $\mathcal{K}_0 \leftarrow \mathcal{K}_0 \setminus \cup_i^{j-1}\mathcal{K}_i$
  $j \leftarrow j + 1$
end while
$J = j - 1$
$Z =$ least common multiple $(|\mathcal{K}_1|, |\mathcal{K}_2|, \cdots, |\mathcal{K}_J|)$
Divide the $\tau_c - \tau_p$ samples into Z equal slot intervals.
In each slot $z,\ z = 1, \ldots, Z$, schedule J UEs, where each UE is from each set $\mathcal{K}_j,\ j = 1, \ldots, J$.

IV. User Scheduling

One can increase the aperture length of the UPA to improve the orthogonality of the channel between the UEs, but this is practically limited by the physical structure of the BS. Thus, to avoid severe interference from the UEs which are not separated enough, the BS needs to schedule those UEs in orthogonal time/frequency slots [15], [16]. Let $\mathbf{\Gamma} = [\gamma_{kk'}] \in \mathbb{C}^{K\times K}$ with $\gamma_{kk'} = \frac{|\hat{\mathbf{g}}_k^{\mathrm{H}}\hat{\mathbf{g}}_{k'}|}{\|\hat{\mathbf{g}}_k\|\|\hat{\mathbf{g}}_{k'}\|}$ be a matrix that captures the correlation of the channels between the UEs. If $\mathbf{\Gamma} \to \mathbf{I}_K$ as $M \to \infty$, then we have channel hardening and favorable propagation [8], [12] and all the UEs can be multiplexed in the same time-frequency slots. However, for long-distance communication scenario some channel vectors can be nearly parallel if the those UEs fall in the same angular window of the main lobe of the BS. We use a heuristic algorithm to group the UEs with nearly parallel channels, where for two UEs k and k', if $\gamma_{kk'} > \gamma_{\text{th}}$, then both UEs are scheduled in different slots, where γ_{th} is threshold correlation value and a design parameter. The user scheduling algorithm is described in Algorithm 1. Thus, with user scheduling at the BS, we remove the UEs causing severe interference, thereby improving the achievable rates to the UEs.

V. Simulation Results

The parameters considered for simulation are tabulated in Table II. The number of clusters considered is $N_{cl} = 10$ and the cluster dependent gain parameter is considered a uniform random variable with gains ranging from 0 dB to 10 dB. As the channel seen by the BS is through a narrow angular interval and dominated by LoS path, we could assume that the channel remains static for a longer time and, hence, allow us to have a larger coherence interval.

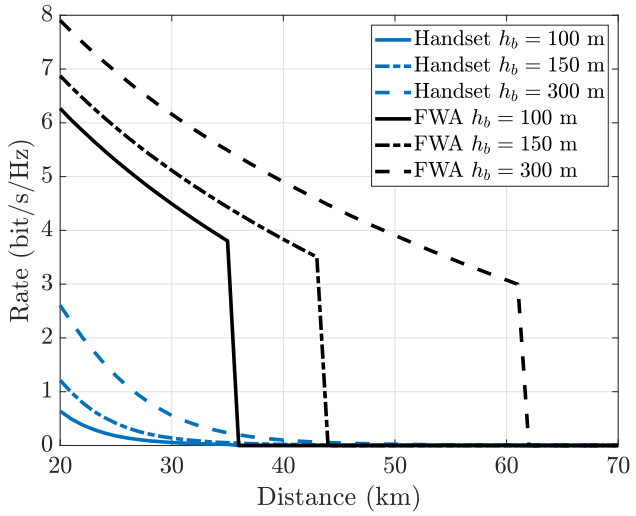

Fig. 1: Coverage range for handset and FWA.

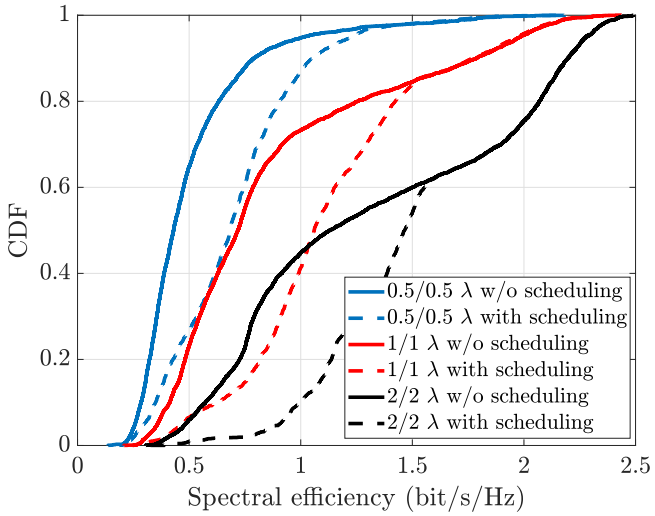

Fig. 2: Rates achieved by users with different antenna spacings at the BS and, with and without user scheduling. Legend to be read as horizontal/vertical spacing in terms of λ.

TABLE II: Simulation Parameters

Frequency of operation, f	3.5 GHz
Bandwidth	100 MHz
UPA configuration	100×10
BS transmit power	100 W
BS noise figure	4.5 dB
Antenna separation horizontal/vertical	2/2 λ
UE noise figure	7 dB
Temperature	300 K
Pilot length τ_p	2000
Coherence length τ_c	15000

A. Coverage

In this subsection, we look at the coverage range that an elevated BS can provide. Consider a single UPA panel in the network and consider a single UE in the direction of the main lobe of the panel. We consider two types of users; (i) a mobile handset with no directional gain (0 dBi) using a class-2 power amplifiers transmitting at maximum power of 500 mW at being located at heights less than 2 m above the ground; (ii) a FWA terminal mounted on at a height of 10 m above the ground with a directional gain antenna of 6 dBi transmitting at a maximum transmit power of 40 dBm. The coverage range for an elevated BS is plotted in Fig. 1 for a mobile handset and FWA. From the plot, we can observe that with the increase in the BS height, the coverage range is increased. The sharp drop in the rates is due to the fact that the BS will be unable to see the UE above the horizon when the maximum range is reached. A mobile handset being used at shorter heights and at lower power faces severe pathloss and lower antenna gain and, hence, the channel estimation quality reduces drastically. Thus, a mobile handset is limited by SNR to achieve higher rates while an FWA is limited by the maximum range which BS can see the UE above the horizon. SuperCell massive MIMO can deliver upto 300 Mbps broadband rates at 60 km distance by using elevated BS.

B. Base Station Requirements

In this subsection, we look at the requirements at the BS to provide broadband access at long distances. To mimic a small village in a rural area, consider a 2×2 km^2 area at 30 km distance in the X-direction from the BS. Fig. 2 shows the rates achieved by 10 uniformly distributed FWA users in the said area with a single panel at the BS. For simulations, we consider $\gamma_{\text{th}} = 0.6$. It can be seen that with an increase in the antenna aperture, the rates also increase owing to the fact that the channels become more resolvable at the BS. By building a UPA with larger aperture or increasing the array antenna spacing, the angular width of the main lobe of the BS will reduce and aids to get less parallel channels between nearby UEs. In this scenario grating lobes (created by the larger aperture) is good in the sense that we redistribute the interference power somewhere else than the area where the user of interest lies in. By implementing user scheduling algorithm, the UEs which are nearby will be scheduled in orthogonal slots, thereby further improving the user achievable rates. This can be observed from the plots with user scheduling as the tail of CDF gets pushed towards right (dashed curves).

C. Sum Rate Analysis

In this section, we analyze the rate achievable by UEs in the SuperCell network. To provide coverage to 360° around the BS, we consider 3 UPA panels each of equipped with an 100×10 array pointing in 0°, 120° and 240°. We consider two user deployment scenarios; (i) UEs are uniformly distributed in an annulus of 20 km to 30 km from the BS; (ii) UEs are uniformly distributed in 3 remote villages of area 5×5 km^2 at 30 km distance from the BS. Zero-forcing operations does not yield good rates as we are operating in noise-limited

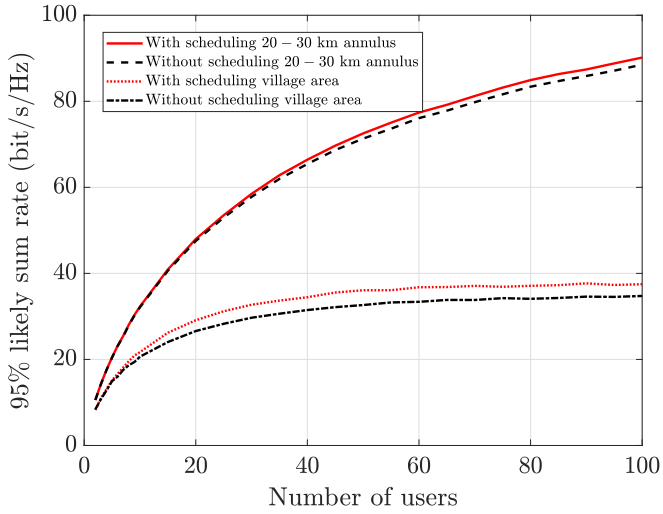

Fig. 3: 95% likely sum rate obtained by FWA users distributed 360° around the BS equipped with 3 panels of 100x10 UPA.

regimes. Thus, we consider maximum-ratio precoding with equal power allocation. The sum-rate achieved by all the users are plotted in Fig. 3. The achievable rate reduces when users are distributed in local regions compared to uniformly distributed users in the cell area due to the reduction of the channel orthogonality between the users. Moreover, note that scheduling is only needed when the users are clustered into a few local regions which can be seen from the gap between sum-rates for scheduled and non-scheduled cases between two user deployment scenarios. It is to be expected in practice that users will be confined to few local regions instead of being uniformly distributed and user scheduling algorithm helps to improve the rates in such cases.

VI. Conclusion

Broadband access is becoming a necessity rather than a luxury in rural areas all around the world. However, due to the low return on investment, ISPs have shown limited interest in providing services in rural areas using conventional cellular technology. There is a need for alternative approaches to providing broadband access over long distances at a low cost. SuperCell massive MIMO using highly elevated BSs with large-aperture antenna arrays is a prospective candidate to bridge the digital divide. This paper investigated this technology, including different aspects to consider when designing a long-range communication system. The elevated BS sees the signal from a UE in a narrow angular interval, thus rich-scattering Rayleigh fading models may not be accurate. We used a cluster-based channel model considering local scattering near the UEs. We investigated the minimum distance criterion between the UEs to resolve them using beamforming. With large-aperture arrays the angular width of the main lobe is reduced and grating lobes might be preferable to improve the spatial resolution. Moreover, implementing a user scheduling algorithm at the BS can further improve the achievable rates by scheduling the UEs having nearly parallel channels in orthogonal slots. Our link budget analysis shows that the coverage range of mobile handsets will be limited by the SNR in large coverage scenarios, while FWA terminals will be limited by the LoS distance seen over the horizon. The simulation results show that we can provide high cell throughput and broadband access services to FWA users over tens of kilometers by using SuperCell massive MIMO.

References

[1] T. L. Marzetta, "Noncooperative cellular wireless with unlimited numbers of base station antennas," *IEEE Trans. on Wireless Commun.*, vol. 9, no. 11, pp. 3590–3600, 2010.

[2] Y. Zhang, D. J. Love, J. V. Krogmeier, C. R. Anderson, R. W. Heath, and D. R. Buckmaster, "Challenges and opportunities of future rural wireless communications," *IEEE Communications Magazine*, vol. 59, no. 12, pp. 16–22, 2021.

[3] L. L. Mendes, C. S. Moreno, M. V. Marquezini, A. M. Cavalcante, P. Neuhaus, J. Seki, N. F. T. Aniceto, H. Karvonen, I. Vidal, F. Valera *et al.*, "Enhanced remote areas communications: The missing scenario for 5G and beyond 5G networks," *IEEE Access*, vol. 8, pp. 219 859–219 880, 2020.

[4] E. Yaacoub and M.-S. Alouini, "A key 6G challenge and opportunity—connecting the base of the pyramid: A survey on rural connectivity," *Proceedings of the IEEE*, vol. 108, no. 4, pp. 533–582, 2020.

[5] P. Bondalapati, A. Tiwari, M. E. Sahin, Q. Tang, S. Saraswat, V. Suryakumar, A. Yazdan, J. Kusuma, and A. Dubey, "SuperCell: A wide-area coverage solution using high-gain, high-order sectorized antennas on tall towers," *arXiv preprint arXiv:2012.00161*, 2020.

[6] R. K. Luneburg, *Mathematical theory of optics*. University of California Press, 2021.

[7] G. P. Fettweis and H. Boche, "6G: The personal tactile internet-and open questions for information theory," *IEEE BITS the Information Theory Magazine*, 2021.

[8] T. L. Marzetta, E. G. Larsson, H. Yang, and H. Q. Ngo, *Fundamentals of massive MIMO*. Cambridge University Press, 2016.

[9] T. Taheri, R. Nilsson, and J. van de Beek, "The potential of massive-MIMO on TV towers for cellular coverage extension," *Wireless Communications and Mobile Computing*, vol. 2021, 2021.

[10] C. A. Balanis, *Antenna Theory: Analysis and Design*. John Wiley & sons, 2016.

[11] U. K. Ganesan, E. Björnson, and E. G. Larsson, "Radioweaves for extreme spatial multiplexing in indoor environments," in *54th Asilomar Conference on Signals, Systems, and Computers*. IEEE, 2020, pp. 1007–1011.

[12] E. Björnson, J. Hoydis, and L. Sanguinetti, *Massive MIMO networks: Spectral, energy, and hardware efficiency*. Now Publishers Inc. Hanover, MA, USA, 2017.

[13] P. Begovic, N. Behlilovic, and E. Avdic, "Applicability evaluation of Okumura, Ericsson 9999 and winner propagation models for coverage planning in 3.5 GHZ WiMAX systems," in *19th International Conference on Systems, Signals and Image Processing (IWSSIP)*. IEEE, 2012, pp. 256–260.

[14] J. Lun, P. Frenger, A. Furuskar, and E. Trojer, "5G New radio for rural broadband: How to achieve long-range coverage on the 3.5 GHz band," in *IEEE 90th Vehicular Technology Conference (VTC2019-Fall)*. IEEE, 2019, pp. 1–6.

[15] Z. Chen, E. Björnson, and E. G. Larsson, "When is the achievable rate region convex in two-user massive MIMO systems?" *IEEE Wireless Communications Letters*, vol. 7, no. 5, pp. 796–799, 2018.

[16] R. S. Chaves, M. V. Lima, E. Cetin, and W. A. Martins, "User selection for massive MIMO under line-of-sight propagation," *IEEE Open Journal of the Communications Society*, 2022.